Inorganic Chemistry
Cite This: Inorg. Chem. 2018, 57, 2193−2198
Article
pubs.acs.org/IC

Robust Bifunctional Lanthanide Cluster Based Metal−Organic Frameworks (MOFs) for Tandem Deacetalization−Knoevenagel Reaction

Yue Zhang,[†] Yuxiang Wang,[‡] Lin Liu,*[,†] Na Wei,[†] Ming-Liang Gao,[†] Dan Zhao,[‡] and Zheng-Bo Han*[,†]

[†]College of Chemistry, Liaoning University, Shenyang 110036, People's Republic of China
[‡]Department of Chemical & Biomolecular Engineering, National University of Singapore, 117585, Singapore

Supporting Information

ABSTRACT: A series of 12-connected lanthanide cluster based metal−organic frameworks (MOFs) have been constructed by $[Ln_6(\mu_3\text{-}OH)_8(COO-)_{12}]$ secondary building units (SBUs) and 2-aminobenzenedicarboxylate (BDC-NH_2) ligands. These obtained materials exhibit high chemical stability and generic thermal stability, especially in acidic and basic conditions. They also present commendable CO_2 adsorption capacity, and Yb-BDC-NH_2 was further confirmed by a breakthrough experiment under both dry and wet conditions. Moreover, these materials possess both Lewis acid and Brønsted base sites that can catalyze one-pot tandem deacetalization−Knoevenagel condensation reactions.

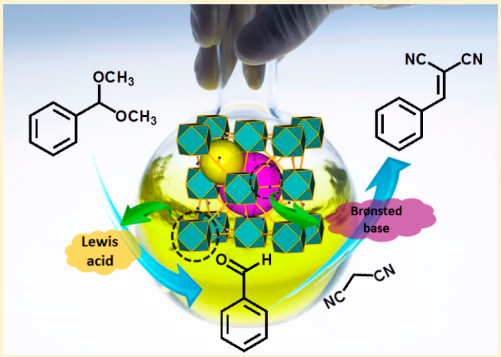

1. INTRODUCTION

Recent years, metal−organic frameworks (MOFs) have been intensely studied as heterogeneous catalysts and applied in the field of organic chemistry, mainly because they possess extremely high surface areas, tunable pore size, and recoverability, as well as a wide range of accessible catalytic sites.[1−6] Stability and catalytic activity are important features for catalysts, which can be found in some MOFs. For instance, MIL-53(Al), UiO-66, UiO-67, UiO-68, and ZIF-8 are undecomposed at temperatures lower than 500 °C and are stable in common organic solvents.[7−9] In addition, polynuclear lanthanide (Ln) cluster based MOFs, showing high stability and good catalytic activity, have been applied in various fields.[10−12] Ln clusters assembled with multifunctional organic ligands can be used in an efficient strategy to design MOFs with special functions. Currently, a few polynuclear Ln cluster based MOFs have been reported with noticeable catalytic activities.[13−15]

Tandem reactions are economical, efficient, and environmentally friendly chemical methods and have been attracting widespread research interest.[16−18] Tandem reactions are sequentially carried out with two or multiple individual reactions in one pot, which can reduce the use of chemicals, mitigate the generation of pollutants, and shorten reaction time.[19] In the organocatalytic field, the development of tandem reactions has become a new direction to offer opportunities for improving chemical transformations, such as hydrogenation reactions, alkene metathesis, and Michael/Morita−Baylis−Hillman reactions.[20−22] Recently, some MOFs have been reported to be high-performance catalysts for tandem reactions.[23−27] For example, the Zhou group reported a Cu paddlewheel-based MOF, denoted PCN-124, to be an excellent catalyst for one-pot tandem deacetalization−Knoevenagel condensations reaction for the synthesis of benzylidene malononitrile.[28]

In our previous work, a series of trinuclear, pentanuclear, and hexanuclear Ln cluster based MOFs were designed and synthesized.[15,29,30] Among these, trinuclear and pentanuclear Ln cluster based MOFs gave preeminent catalytic activity toward the cycloaddition of CO_2 and epoxides, hexanuclear Ln cluster based MOFs possessed luminescence, and all showed good stability. In this work, a series of 12-connected hexanuclear Ln (Ln = Yb, Dy, Sm) cluster based MOFs incorporating $[Ln_6(\mu_3\text{-}OH)_8(COO-)_{12}]$ and an amino-functionalized ligand (2-aminobenzenedicarboxylate, BDC-NH_2) have been synthesized by solvothermal reactions with the formula $[(CH_3)_2NH_2]_2[Ln_6(\mu_3\text{-}OH)_8(BDC\text{-}NH_2)_6(H_2O)_6]\cdot x(solv)$ (Ln = Yb, Dy, Sm) (Figure 1). These compounds show high chemical stability and generic thermal stability in common organic solvents and water with pH values ranging from 2 to 12. Due to the existence of $-NH_2$ groups, they show high adsorption capacity for CO_2. In addition, the CO_2 adsorption capacity of Yb-BDC-NH_2 was further studied by breakthrough experiments under both dry and wet conditions. More strikingly, the Ln clusters afford Lewis acid sites and ligands offer Brønsted base sites, making them highly efficient

Received: December 7, 2017
Published: January 31, 2018

DOI: 10.1021/acs.inorgchem.7b03084
Inorg. Chem. 2018, 57, 2193−2198

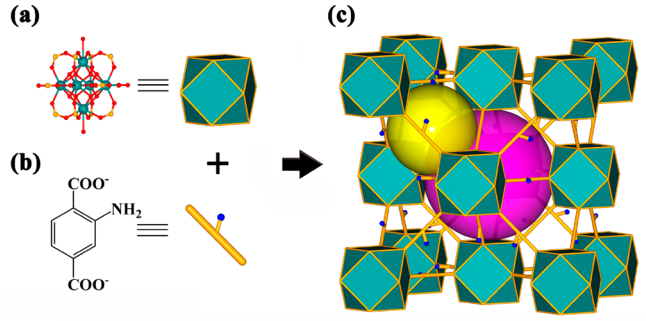

Figure 1. (a) Ball and stick representation of the hexanuclear unit $[Ln_6(\mu_3\text{-}OH)_8(COO)_{12}]$ (yellow. C; red. O; green. Ln). (b) Representation of the BDC-NH_2 ligand. (c) Packing of two types of cages: the tetrahedral cage and the octahedral cage.

bifunctional catalysts for one-pot tandem deacetalization−Knoevenagel condensation reaction.

2. EXPERIMENTAL SECTION

2.1. Materials and Methods. All chemicals for synthesis were commercially available reagents of analytical grade and were used without further purification. C, H, and N microanalyses were carried out with a PerkinElmer 240 elemental analyzer. FT-IR spectra were recorded from KBr pellets in the 4000−450 cm^{-1} range on a Nicolet 5DX spectrometer. Thermogravimetric analyses (TGA) were taken on a PerkinElmer Pyrisl instrument (35−800 °C, 5 °C min^{-1}, flowing N_2 gas). Powder X-ray diffraction was recorded with a Bruker D8 ADVANCE automated diffractometer with Cu Kα radiation. Variable-temperature PXRD studies were conducted by heating the sample at a constant rate of 5 °C min^{-1} from room temperature to 100, 150, 200, 250, 300, and 350 °C in air, respectively. The products of catalysis reactions were monitored by ^{1}H NMR spectra recorded on a Varian 300 MHz NMR spectrometer.

N_2 sorption isotherms were measured at 77 K using a liquid-N_2 bath. CO_2 sorption isotherms were measured at 273 K using an ice/water bath and at 298 K using a water bath. N_2 and CO_2 adsorption−desorption experiments were carried out on an automated gas sorption analyzer (Quantachrome Instruments ASiQC). The samples of Yb-BDC-NH_2, Dy-BDC-NH_2, and Sm-BDC-NH_2 were activated by washing the as-synthesized crystals with DMF followed by solvent exchange in CH_3OH and CH_2Cl_2 for 3 days, respectively. The solution was refreshed several times daily during this period. In a typical experiment, 80−100 mg of each activated sample was transferred (dry) to a 6 mm large bulb glass sample cell and was first evacuated at room temperature using a turbo molecular vacuum pump and then gradually heated to 150 °C to hold for 24 h and cooled to room temperature.

Breakthrough experiments were carried out using a home-built setup coupled with a mass spectrometer (Hiden QGA). A dry powder of Yb-BDC-NH_2 (500 mg for 7 cm column) was packed in a stainless steel column with a diameter of 0.635 cm as the adsorbent bed. The packed column was heated at 120 °C for 12 h under a constant He flow (4 ± 0.5 cm^3 min^{-1} at 298 K and 2 bar) to activate the MOF. After that, a mixed gas containing CO_2/N_2 (15/85) with a flow rate of 4.75 ± 0.75 cm^3 min^{-1} (298 K, 2 bar) was introduced to the column. Breakthrough tests of CO_2 and N_2 (15 ± 0.5)/(85 ± 0.5) mixtures under wet conditions (80 ± 5% RH) were also carried out.[31]

2.2. Synthesis of Compounds. *2.2.1. Synthesis of Yb-BDC-NH_2, $[(CH_3)_2NH_2]_2[Yb_6(\mu_3\text{-}OH)_8(BDC\text{-}NH_2)_6(H_2O)_6]\cdot x(solv)$ (1).* A mixture of H_2BDC-NH_2 (9.0 mg, 0.05 mmol), $Yb(NO_3)_3\cdot 6H_2O$ (19.3 mg, 0.04 mmol), and 2-fluorobenzoic acid (48.7 mg) were dissolved in 2.9 mL of a mixed solvent of DMF (2.2 mL), H_2O (0.5 mL), and HNO_3 (0.2 mL, 3.57 M in DMF) in a 3.5 mL scintillation vial. The resulting mixture was kept in an oven at 105 °C for 72 h. After the vial was cooled to room temperature, the as-synthesized sample was purified through repeated washing with DMF to yield khaki octahedral crystals. Yield: 63% (based on the crystals dried in air). Anal. Calcd for $C_{52}H_{66}Yb_6N_8O_{38}$: C, 25.50; H, 2.72; N, 4.57. Found: C, 25.74; H, 2.69; N, 4.61.

2.2.2. Synthesis of Dy-BDC-NH_2, $[(CH_3)_2NH_2]_2[Dy_6(\mu_3\text{-}OH)_8(BDC\text{-}NH_2)_6(H_2O)_6]\cdot x(solv)$ (2). The synthesis process of **2** was similar to that of **1** except with $Dy(NO_3)_3\cdot 6H_2O$ instead of ytterbium nitrate. Yield: 68% (based on the crystals dried in air). Anal. Calcd for $C_{52}H_{66}Dy_6N_8O_{38}$: C, 27.00; H, 2.88; N, 4.84. Found: C, 26.97; H, 2.90; N, 4.86.

2.2.3. Synthesis of Sm-BDC-NH_2, $[(CH_3)_2NH_2]_2[Sm_6(\mu_3\text{-}OH)_8(BDC\text{-}NH_2)_6(H_2O)_6]\cdot x(solv)$ (3). The synthesis process of **3** was similar to that of **1** except with $Sm(NO_3)_3\cdot 6H_2O$ instead of ytterbium nitrate. Yield: 72% (based on the crystals dried in air). Anal. Calcd for $C_{52}H_{66}Sm_6N_8O_{38}$: C, 26.17; H, 2.79; N, 4.70. Found: C, 26.21; H, 2.76; N, 4.66.

2.3. X-ray Crystallography. Crystallographic data of Yb-BDC-NH_2, Dy-BDC-NH_2, and Sm-BDC-NH_2 were collected at 173 K with a Bruker D8 Quest diffractometer with Mo Kα radiation (λ = 0.71073 Å) and a graphite monochromator using the ω-scan mode. All measured intensities were corrected for Lorentz and polarization effects. Absorption corrections were applied using the programs SADABS and HABITUS.[32,33] The structure was solved by direct methods and refined on F^2 by full-matrix least squares using the SHELXTL-2014 crystallographic software package.[34] Non-hydrogen atoms were treated anisotropically. Positions of hydrogen atoms were generated geometrically. There is a large solvent-accessible pore volume in the structures of Yb-BDC-NH_2, Dy-BDC-NH_2, and Sm-BDC-NH_2, which is occupied by highly disordered solvent molecules. No satisfactory disorder model for these solvent molecules could be achieved, and therefore the SQUEEZE program implemented in PLATON was used to remove these electron densities of these disordered species.[35] Crystallographic data for structural analyses are summarized in Table S1. The CCDC reference numbers are 1569272, 1569273, and 1569274 for Yb-BDC-NH_2, Dy-BDC-NH_2, and Sm-BDC-NH_2, respectively.

2.4. Catalytic Performance Evaluation. Before the reactions, the catalysts were activated at 298 K for 24 h under vacuum to remove the residual solvent molecules on the surface of MOFs. The catalytic reactions were carried out in a 10 mL reaction tube using benzaldehyde dimethyl acetal (2.0 mmol) and malononitrile (2.1 mmol) in DMSO-d_6 (2.0 mL) with magnetic stirring. Catalysts (100 mg) were then added and maintained at 50 °C for 24 h under a N_2 atmosphere. When the reaction was completed, the reactor was cooled to room temperature. The products were monitored by ^{1}H NMR. The catalysts were separated by filtration, washed abundantly with CH_3OH, placed in a vial, and soaked in CH_3OH for 4 h and subsequently dried under vacuum at room temperature and then reused in the recycle reaction.

3. RESULTS AND DISCUSSION

3.1. Crystal Structure. Compounds Yb-BDC-NH_2, Dy-BDC-NH_2, and Sm-BDC-NH_2 are isostructural with the previously reported Eu-based MOF (Eu-BDC-NH_2),[36] which is also constructed by hexanuclear Ln clusters and BDC-NH_2 linkers with fcu topology. Thus, only the crystal structure of Yb-BDC-NH_2 is simply described here. Single-crystal X-ray crystallography indicates that Yb-BDC-NH_2 crystallizes in the cubic space group $Fm\bar{3}m$. Twelve-connected hexanuclear SBUs are linked by BDC-NH_2 ligands to form the 3D framework enclosing two types of polyhedral cages: octahedral and tetrahedral (Figure 1). The empirical chemical formula is $[(CH_3)_2NH_2]_2[Yb_6(\mu_3\text{-}OH)_8(BDC\text{-}NH_2)_6(H_2O)_6]\cdot 11DMF$, which was estimated by ^{1}H NMR measurements for digested Yb-BDC-NH_2 crystals in DCl/D_2O/DMSO (Figure S1).

3.2. Chemical and Thermal Stability. The compounds Yb-BDC-NH_2, Dy-BDC-NH_2, and Sm-BDC-NH_2 possess high chemical stability and general thermal stability. The chemical stability tests were carried out by soaking the samples in various organic solvents (methanol, ethanol, dichloromethane, 1,4-

DOI: 10.1021/acs.inorgchem.7b03084
Inorg. Chem. 2018, 57, 2193−2198

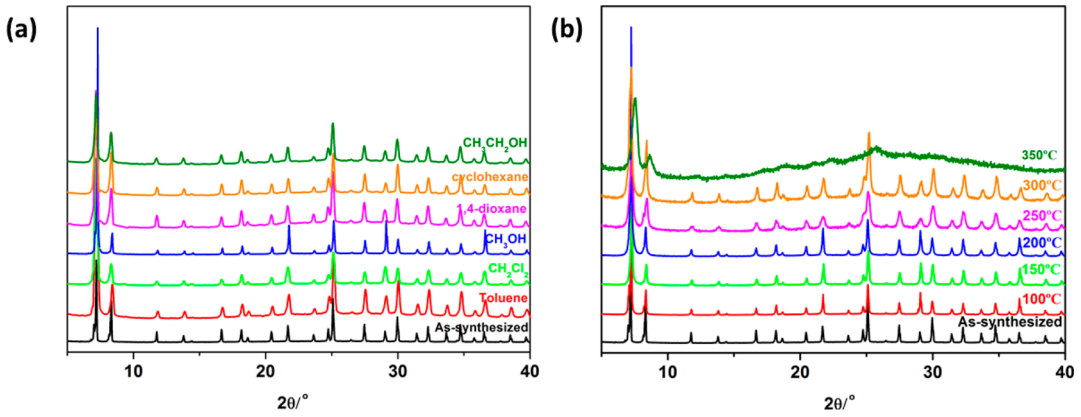

Figure 2. (a) PXRD patterns of Yb-BDC-NH_2 soaked in various organic solvents for 24 h. (b) Thermal stability tests for Yb-BDC-NH_2 monitored by variable-temperature PXRD analysis.

dioxane, cyclohexane, toluene), water, and even acidic and basic solutions (i.e., HCl (pH 2) and NaOH (pH 12)) for 24 h. The unaltered PXRD patterns of three compounds indicate no framework collapse or phase transition during these tests (Figure 2a and Figures S2 and S4–S6). The thermal stability was investigated by variable-temperature PXRD and thermogravimetric analysis (TGA). The results confirm that these compounds are stable up to 300 °C in air (Figure 2b and Figures S3–S7).

3.3. FT-IR Spectra. The IR spectra (Figure S8) of Yb-BDC-NH_2, Dy-BDC-NH_2, and Sm-BDC-NH_2 exhibit characteristic bands of carboxyl groups at 1664 and 1572 cm^{-1} for the antisymmetric stretching vibrations and at 1430 and 1384 cm^{-1} for the symmetric stretching vibrations.[37] The separations (Δ) between $\nu_{asym}(CO_2)$ and $\nu_{sym}(CO_2)$ indicate the presence of bidentate bridging coordination modes in the three compounds (234 and 188 cm^{-1}).[38] In addition, the asymmetric and symmetric $-NH_2$ absorption bands at 3428 and 3344 cm^{-1} as well as the N–H bending vibration at 1621 cm^{-1} and the C–N stretching vibration absorption bands at 1257 cm^{-1} confirm that free $-NH_2$ groups exist in the three compounds.[39,40]

3.4. Gas Sorption. N_2 sorption isotherms (Figure 3) of Yb-BDC-NH_2, Dy-BDC-NH_2, and Sm-BDC-NH_2 at 77 K display a fully reversible type I shape, confirming their microporosity. Utilizing the BET (Brunauer–Emmett–Teller) method, the surface areas of Yb-BDC-NH_2, Dy-BDC-NH_2, and Sm-BDC-NH_2 were calculated to be 107.7, 148.2, and 171.7 $m^2\ g^{-1}$, respectively.

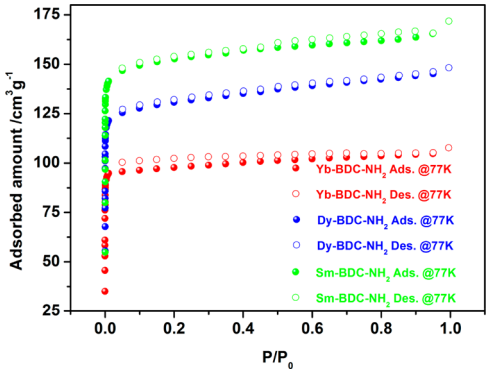

Figure 3. N_2 adsorption/desorption isotherms of Yb-BDC-NH_2, Dy-BDC-NH_2, and Sm-BDC-NH_2 at 77 K.

In order to verify the ligand functionalization effect of the three compounds, the CO_2 sorption capacities of Yb-BDC-NH_2, Dy-BDC-NH_2, and Sm-BDC-NH_2 were evaluated (Figure 4). When the total pressure of CO_2 gets close to 760 Torr, the CO_2 uptakes reach 57.3, 79.1, and 112.3 $cm^3\ g^{-1}$ at 273 K, respectively, which are higher than those of a few reported MOFs possessing multinuclear metal cluster moieties at the same pressure, such as PCN-56 (ca. 55 $cm^3\ g^{-1}$) and Y-ftw-MOF-2 (ca. 56 $cm^3\ g^{-1}$),[41,42] but lower than that for fcu-MOF (ca. 134 $cm^3\ g^{-1}$).[43] At 298 K, the CO_2 uptakes of Yb-BDC-NH_2, Dy-BDC-NH_2, and Sm-BDC-NH_2 could reach 35.6, 41.2, and 59.0 $cm^3\ g^{-1}$, respectively. The isosteric heat of adsorption (Q_{st}) was calculated on the basis of the CO_2 adsorption isotherms at 273 and 298 K using the Clausius–Clapeyron equation,[44] revealing that Q_{st} values of Yb-BDC-NH_2, Dy-BDC-NH_2, and Sm-BDC-NH_2 at zero surface coverage are 13.3, 20.3, and 27.4 kJ mol^{-1}, respectively. The amino-functionalized MOFs have a higher CO_2 adsorption energy, which could be mainly attributed to a stronger interaction between CO_2 and the amino groups in the pores.[45] The formation of electron donor–acceptor complexes between CO_2 and the amino-functionalized MOF structure may have an effect on the CO_2 sorption.[46]

3.5. Breakthrough Experiments. The coadsorption of the mixed gas N_2/CO_2 in Yb-BDC-NH_2 was completed by using dynamic column breakthrough tests under both dry and wet conditions.

Typically, a longer breakthrough time represents a higher gas uptake capacity, and a greater difference of breakthrough time among various gas components indicates better gas separation performance. Under dry conditions, the CO_2 breakthrough time of Yb-BDC-NH_2 is around 500 s (Figure 5). To estimate the breakthrough time in the presence of water, we introduced a gas mixture containing 15 ± 1% of dry CO_2 and 85 ± 1% of wet N_2 (80 ± 5% RH) to the MOF-packed column. The breakthrough time of Yb-BDC-NH_2 under wet conditions showed an almost 80% decrease in comparison to that in the absence of moisture (Figure S9). This can be attributed to the open metal sites in this MOF that were occupied by water molecules under humid conditions, leading to reduced CO_2 sorption site and therefore reduced CO_2 uptake capacity.[47,48] Therefore, water has some influence on the CO_2 uptake in Yb-BDC-NH_2.

3.6. Catalytic Deacetalization–Knoevenagel Reaction. Yb-BDC-NH_2, Dy-BDC-NH_2, and Sm-BDC-NH_2 contain Ln

DOI: 10.1021/acs.inorgchem.7b03084
Inorg. Chem. 2018, 57, 2193–2198

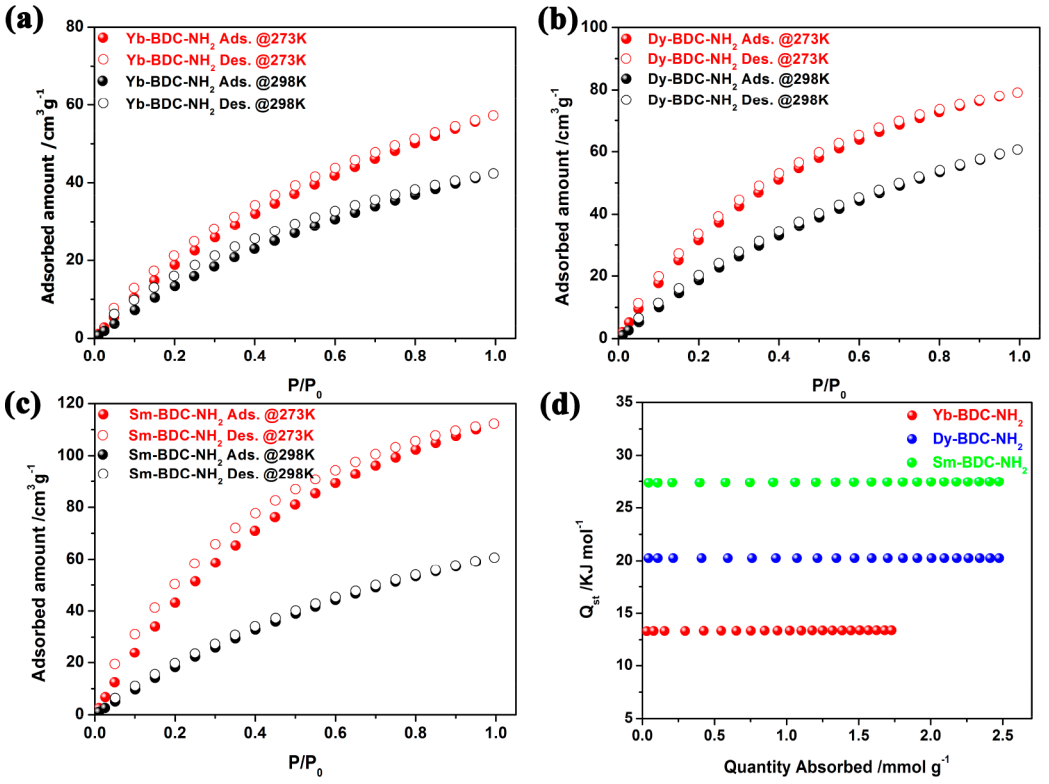

Figure 4. (a) Adsorption/desorption isotherms of CO_2 (273 and 298 K) for Yb-BDC-NH_2. (b) Adsorption/desorption isotherms of CO_2 (273 and 298 K) for Dy-BDC-NH_2. (c) Adsorption/desorption isotherms of CO_2 (273 and 298 K) for Sm-BDC-NH_2. (d) Isosteric heats of CO_2 adsorption (Q_{st}) of the three compounds calculated from the adsorption isotherms at 273 and 298 K.

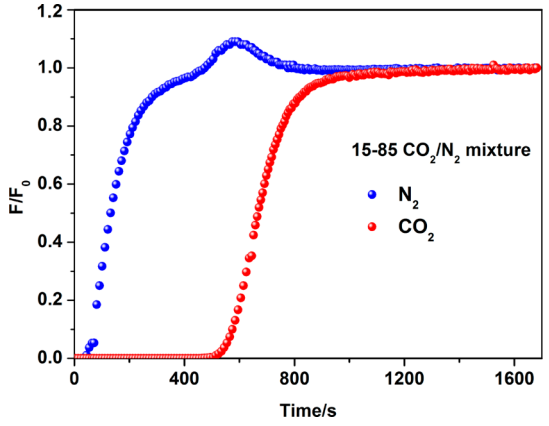

Figure 5. Breakthrough curves of a CO_2/N_2 mixture in Yb-BDC-NH_2 with a total CO_2/N_2 mixture flow rate of 4.75 ± 0.25 cm^3 min^{-1} (P = 2 bar) at 298 K.

Table 1. One-Pot Deacetalization–Knoevenagel Condensation Reactions and Yields[a]

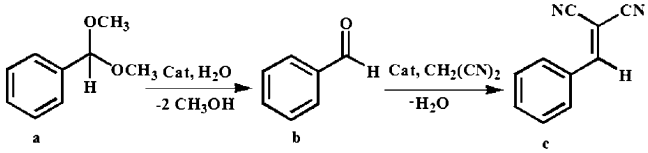

entry	conversn of **a** (%)	yield of **b** (%)	yield of **c** (%)
Yb-BDC-NH_2	97.0	trace	97.0
Dy-BDC-NH_2	82.0	trace	82.0
Sm-BDC-NH_2	76.0	trace	76.0
second recycle	93.0	2.7	90.3
third recycle	92.0	0.4	91.6
fourth recycle	90.2	0.2	90.0
no catalyst	~0	trace	trace

[a]Reaction conditions: benzaldehyde dimethyl acetal (2.0 mmol), malononitrile (2.1 mmol), DMSO-d_6 (2 mL), and catalyst (100 mg); reaction temperature 50 °C; reaction time 24 h. The conversions were determined by ^{1}H NMR.

ions which possess Lewis acidic activity to catalyze the deprotection of benzaldehyde dimethyl acetal to give benzaldehyde. An amino group as a weak Brønsted base can catalyze the Knoevenagel condensation reaction between benzaldehyde and malononitrile (Table 1). The amino groups undergo nucleophilic attack on the carbonyl carbon, and water is released in the formation of an imine intermediate. Then, malononitrile reacts with the intermediate. Finally, products are formed and the amino groups are regenerated.[49] Thus, the three compounds are a kind of potential bifunctional acid–base catalyst. In order to prove this point, Yb-BDC-NH_2, Dy-BDC-NH_2, and Sm-BDC-NH_2 were utilized to study their catalytic activity for tandem deacetalization–Knoevenagel condensation reactions.

The catalytic reactions were performed with 2 mmol of each substrate in DMSO-d_6 (2 mL) an the catalyst (100 mg) in a 10 mL reaction tube at 50 °C under a N_2 atmosphere for 24 h. ^{1}H NMR spectroscopy was utilized to detect this tandem reaction process. Experimental results are given in Table 1. After 24 h of reaction, the yields of product **c** catalyzed by Yb-BDC-NH_2, Dy-BDC-NH_2, and Sm-BDC-NH_2 reach about 97.0, 82.0, and 76.0%, respectively. In comparison with previous catalysts (Table S2), the three compounds also exhibit good catalytic

DOI: 10.1021/acs.inorgchem.7b03084
Inorg. Chem. 2018, 57, 2193–2198

activity toward the deacetalization−Knoevenagel condensation reaction. Among them, Yb-BDC-NH_2 demonstrates the highest catalytic activity due to the smaller ionic radius and stronger Lewis acidity[50] (Table 1). Hence, Yb-BDC-NH_2 was chosen to explore the dynamic change of the reaction over time (Figure S10) and catalyst recovery. Though the activity of catalyst Yb-BDC-NH_2 decreased slightly, it is still better those for than the other two catalysts that were isolated from the reaction suspensions by centrifugation. After four runs of the reaction, the weight and color of the catalyst Yb-BDC-NH_2 were unchanged. Moreover, the PXRD pattern of Yb-BDC-NH_2 after four cycles was still identical with that of the as-synthesized catalyst, indicating that it maintains its structural integrity after catalytic experiments (Figure S11). On the basis of a control experiment, there is no occurrence of a tandem reaction in the absence of catalyst. Hence, the results could prove that Yb-BDC-NH_2 plays an important role in catalyzing tandem deacetalization−Knoevenagel condensation reactions.

4. CONCLUSIONS

A series of bifunctional hexanuclear Ln cluster based MOFs (Ln = Yb, Dy, Sm) has been successfully constructed. These MOFs exhibit high chemical stability and generic thermal stability. The amino-functionalized ligands are helpful to the CO_2 adsorption, which was proven by gas sorption isotherms and dynamic column breakthrough experiments. Moreover, there are both Lewis acid sites and Brønsted base sites in those MOFs, making them bifunctional catalysts in catalyzing tandem deacetalization−Knoevenagel reactions. Among these MOFs, Yb-BDC-NH_2 possesses high activity and superb recyclability without loss of catalytic activity during the reuse cycles. Our future work will deal with systematically synthesizing multifunctional polynuclear Ln cluster based MOFs and exploring their properties in one-pot tandem reactions.

■ ASSOCIATED CONTENT

Supporting Information

The Supporting Information is available free of charge on the ACS Publications website at DOI: 10.1021/acs.inorgchem.7b03084.

Physical characterization data, crystallographic data, and details of catalysis (PDF)

Accession Codes

CCDC 1569272−1569274 contain the supplementary crystallographic data for this paper. These data can be obtained free of charge via www.ccdc.cam.ac.uk/data_request/cif, or by emailing data_request@ccdc.cam.ac.uk, or by contacting The Cambridge Crystallographic Data Centre, 12 Union Road, Cambridge CB2 1EZ, UK; fax: +44 1223 336033.

■ AUTHOR INFORMATION

Corresponding Authors

*E-mail for L.L.: liulin@lnu.edu.cn.
*E-mail for Z.-B.H.: ceshzb@lnu.edu.cn.

ORCID

Dan Zhao: 0000-0002-4427-2150
Zheng-Bo Han: 0000-0001-8635-9783

Notes

The authors declare no competing financial interest.

■ ACKNOWLEDGMENTS

This work was financially supported by the National Natural Science Foundation of China (Grants 21671090, 21701076, and 21271096).

■ REFERENCES

(1) Lee, J. Y.; Farha, O. K.; Roberts, J.; Scheidt, K. A.; Nguyen, S. T.; Hupp, J. T. Metal-Organic Frameworks as Catalysts. *Chem. Soc. Rev.* **2009**, *38*, 1450−1459.

(2) Leenders, S. H.; Gramage-Doria, R.; de Bruin, B.; Reek, J. N. Transition Metal Catalysis in Confined Spaces. *Chem. Soc. Rev.* **2015**, *44*, 433−448.

(3) Huang, Y. B.; Liang, J.; Wang, X. S.; Cao, R. Multifunctional Metal-Organic Framework Catalysts: Synergistic Catalysis and Tandem Reactions. *Chem. Soc. Rev.* **2017**, *46*, 126−157.

(4) Hu, Z.; Zhao, D. Metal-Organic Frameworks with Lewis Acidity: Synthesis, Characterization, and Catalytic Applications. *CrystEngComm* **2017**, *19*, 4066−4081.

(5) Zhou, Z.; He, C.; Xiu, J.; Yang, L.; Duan, C. Metal-Organic Polymers Containing Discrete Single-Walled Nanotube as a Heterogeneous Catalyst for the Cycloaddition of Carbon Dioxide to Epoxides. *J. Am. Chem. Soc.* **2015**, *137*, 15066−15069.

(6) Rogge, S. M.; Bavykina, A.; Hajek, J.; Garcia, H.; Olivossuarez, A. I.; Sepúlvedaescribano, A.; Vimont, A.; Clet, G.; Bazin, P.; Kapteijn, F.; Daturi, M.; Ramos-Fernandez, E. V.; Llabre' s iXamena, F. X.; Van Speybroeck, V.; Gascon, J. Metal-organic and covalent organic frameworks as single-site catalysts. *Chem. Soc. Rev.* **2017**, *46*, 3134−3184.

(7) Loiseau, T.; Serre, C.; Huguenard, C.; Fink, G.; Taulelle, F.; Henry, M.; Bataille, T.; Férey, G. A Rationale for the Large Breathing of the Porous Aluminum Terephthalate (MIL-53) Upon Hydration. *Chem. - Eur. J.* **2004**, *10*, 1373−1382.

(8) Cavka, J. H.; Jakobsen, S.; Olsbye, U.; Guillou, N.; Lamberti, C.; Bordiga, S.; Lillerud, K. P. A New Zirconium Inorganic Building Brick Forming Metal Organic Frameworks with Exceptional Stability. *J. Am. Chem. Soc.* **2008**, *130*, 13850−13851.

(9) Park, K. S.; Ni, Z.; Côté, A. P.; Choi, J. Y.; Huang, R.; Uribe-Romo, F. J.; Chae, H. K.; O'Keeffe, M.; Yaghi, O. M. From the Cover: Exceptional Chemical and Thermal Stability of Zeolitic Imidazolate Frameworks. *Proc. Natl. Acad. Sci. U. S. A.* **2006**, *103*, 10186−10191.

(10) Wang, X. F.; Zhang, Y. B.; Cheng, X. N.; Chen, X. M. Two Microporous Metal-Organic Frameworks with Different Topologies Constructed from Linear Trinuclear $M_3(COO)n$ Secondary Building Units. *CrystEngComm* **2008**, *10*, 753−758.

(11) Alezi, D.; Peedikakkal, A. M.; Weselinski, L. J.; Guillerm, V.; Belmabkhout, Y.; Cairns, A. J. Quest for Highly-Connected MOF Platforms: Rare-Earth Polynuclear Clusters Versatility Meets Net Topology Needs. *J. Am. Chem. Soc.* **2015**, *137*, 5421−5430.

(12) Farrusseng, D.; Aguado, S.; Pinel, C. Metal-Organic Frameworks: Opportunities for Catalysis. *Angew. Chem., Int. Ed.* **2009**, *48*, 7502−7513.

(13) Mitchell, L.; Gonzalez-Santiago, B.; Mowat, J. P. S.; Gunn, M. E.; Williamson, P.; Acerbi, N.; Clarke, M. L.; Wright, P. A. Remarkable Lewis Acid Catalytic Performance of the scandium trimesate metal organic framework MIL-100(Sc) for C-C and C = N bond-forming reactions. *Catal. Sci. Technol.* **2013**, *3*, 606−617.

(14) Guillerm, V.; Weselinski, L.; Belmabkhout, Y.; Cairns, A. J.; D'Elia, V.; Wojtas, L.; Adil, K.; Eddaoudi, M. Discovery and introduction of a (3, 18)-connected net as an ideal blueprint for the design of metal-organic frameworks. *Nat. Chem.* **2014**, *6*, 673−680.

(15) Wei, N.; Zhang, Y.; Liu, L.; Han, Z. B.; Yuan, D. Q. Pentanuclear Yb(III) cluster-based metal-organic frameworks as heterogeneous catalysts for CO_2 conversion. *Appl. Catal., B* **2017**, *219*, 603−610.

(16) Chng, L. L.; Erathodiyil, N.; Ying, J. Y. Nanostructured Catalysts for Organic Transformations. *Acc. Chem. Res.* **2013**, *46*, 1825−1837.

DOI: 10.1021/acs.inorgchem.7b03084
Inorg. Chem. 2018, 57, 2193−2198

(17) Climent, M. J.; Corma, A.; Iborra, S. Mono- and Multisite Solid Catalysts in Cascade Reactions for Chemical Process Intensification. *ChemSusChem* **2009**, *2*, 500−506.
(18) Wasilke, J. C.; Obrey, S. J.; Baker, R. T.; Baza, G. C. Concurrent Tandem Catalysis. *Chem. Rev.* **2005**, *105*, 1001−1020.
(19) Dhakshinamoorthy, A.; Garcia, H. Cascade Reactions Catalyzed by Metal Organic Frameworks. *ChemSusChem* **2014**, *7*, 2392−2410.
(20) Liu, H.; Li, Y.; Luque, R.; Jiang, H. A. Tuneable Bifunctional Water-Compatible Heterogeneous Catalyst for the Selective Aqueous Hydrogenation of Phenols. *Adv. Synth. Catal.* **2011**, *353*, 3107−3113.
(21) Braddock, D. C.; Wildsmith, A. J. On the use of tandem allylic acetate isomerisation and ring-closing metathesis with palladium (0) phosphine complexes and ruthenium benzylidenes as orthogonal catalysts. *Tetrahedron Lett.* **2001**, *42*, 3239−3242.
(22) Cabrera, S.; Alemán, J.; Bolze, P.; Bertelsen, S.; Jørgensen, K. A. An Unexpected Organocatalytic Asymmetric Tandem Michael/Morita-Baylis-Hillman Reaction. *Angew. Chem.* **2008**, *120*, 127−131.
(23) Li, H.; Zhu, Z.; Zhang, F.; Xie, S.; Li, H.; Li, P.; Zhou, X. Palladium Nanoparticles Confined in the Cages of MIL-101: An Efficient Catalyst for the One-Pot Indole Synthesis in Water. *ACS Catal.* **2011**, *1*, 1604−1612.
(24) Bi, H. P.; Liu, X. Y.; Gou, F. R.; Guo, L. N.; Duan, X. H.; Shu, X. Z.; Liang, Y. M. Highly Regioselective Synthesis of Spirocyclic Compounds by a Palladium-Catalyzed Intermolecular Tandem Reaction. *Angew. Chem.* **2007**, *119*, 7198−7201.
(25) Beyzavi, M. H.; Vermeulen, N. A.; Howarth, A. J.; Tussupbayev, S.; League, A. B.; Schweitzer, N. M.; Gallagher, J. R.; Platero-Prats, A. E.; Hafezi, N.; Sarjeant, A. A.; Miller, J. T.; Chapman, K. W.; Stoddart, J. F.; Cramer, C. J.; Hupp, J. T.; Farhaet, O. K. A Hafnium-Based Metal-Organic Framework as a Nature-Inspired Tandem Reaction Catalyst. *J. Am. Chem. Soc.* **2015**, *137*, 13624−13631.
(26) Zhao, M.; Deng, K.; He, L.; Liu, Y.; Li, G.; Zhao, H.; Tang, Z. Y. Core-Shell Palladium Nanoparticle@Metal-Organic Frameworks as Multifunctional Catalysts for Cascade Reactions. *J. Am. Chem. Soc.* **2014**, *136*, 1738−1741.
(27) Chen, Y. Z.; Zhou, Y. X.; Wang, H.; Lu, J.; Uchida, T.; Xu, Q.; Yu, S. H.; Jiang, H. L. Multifunctional PdAg@MIL-101 for One-Pot Cascade Reactions: Combination of Host−Guest Cooperation and Bimetallic Synergy in Catalysis. *ACS Catal.* **2015**, *5*, 2062−2069.
(28) Park, J.; Li, J. R.; Chen, Y. P.; Yu, J.; Yakovenko, A. A.; Wang, Z. U.; Sun, L. B.; Balbuena, P. B.; Zhou, H. C. A versatile metal-organic framework for carbon dioxide capture and cooperative catalysis. *Chem. Commun.* **2012**, *48*, 9995−9997.
(29) Wei, N.; Zuo, R. X.; Zhang, Y. Y.; Han, Z. B.; Gu, X. J. Robust high-connected rare-earth MOFs as efficient heterogeneous catalysts for CO_2 conversion. *Chem. Commun.* **2017**, *53*, 3224−3227.
(30) Gao, M. L.; Wang, W. J.; Liu, L.; Han, Z. B.; Wei, N.; Cao, X. M.; Yuan, D. Q. Microporous Hexanuclear Ln(III) Cluster-Based Metal-Organic Frameworks: Color Tunability for Barcode Application and Selective Removal of Methylene Blue. *Inorg. Chem.* **2017**, *56*, 511−517.
(31) Hu, Z. G.; Wang, Y. X.; Farooq, S.; Zhao, D. A highly stable metal-organic framework with optimum aperture size for CO_2 capture. *AIChE J.* **2017**, *63*, 4103−4114.
(32) Sheldrick, G. M. *SADABS, Program for Adsorption Correction of Area Detector Frames*; University of Göttingen, Göttingen, Germany, 1996.
(33) Herrendorf, W. *HABITUS, Program for Optimization of the Crystal Shape for the Numerical Adsorption Correction*; Universities of Karlsruhe and Gießen, Karlsruhe and Gießen, Germany, 1993/1997.
(34) Sheldrick, G. M. *SHELXS-2014, Program for the solution and refinement of crystal structures*; University of Göttingen, Göttingen, Germany, 2014.
(35) Spek, A. L. Single-crystal structure validation with the program PLATON. *J. Appl. Crystallogr.* **2003**, *36*, 7−13.
(36) Yi, P.; Huang, H.; Peng, Y.; Liu, D.; Zhong, C. A series of europium-based metal organic frameworks with tuned intrinsic luminescence properties and detection capacities. *RSC Adv.* **2016**, *6*, 111934−111941.
(37) Gao, W. Y.; Wu, H.; Leng, K.; Sun, Y.; Ma, S. Inserting CO_2 into Aryl C-H Bonds of Metal-Organic Frameworks: CO_2 Utilization for Direct Heterogeneous C-H Activation. *Angew. Chem., Int. Ed.* **2016**, *55*, 5472−5476.
(38) Zhang, M. Y.; Shan, W. J.; Han, Z. B. Syntheses and magnetic properties of three Mn(II) coordination polymers based on a tripodal flexible ligand. *CrystEngComm* **2012**, *14*, 1568−1574.
(39) Modrow, A.; Zargarani, D.; Herges, R.; Stock, N. Introducing a photo-switchable azo-functionality inside Cr-MIL-101-NH_2 by co-valent post-synthetic modification. *Dalton Trans.* **2012**, *41*, 8690−8696.
(40) Kandiah, M.; Usseglio, S.; Svelle, S.; Olsbye, U.; Lillerud, K. P.; Tilset, M. Post-synthetic modification of the metal−organic framework compound UiO-66. *J. Mater. Chem.* **2010**, *20*, 9848−9851.
(41) Luebke, R.; Belmabkhout, Y.; Weseliński, Ł. J.; Cairns, A. J.; Alkordi, M.; Norton, G.; Wojtas, Ł.; Adila, K.; Eddaoudi, M. Versatile rare earth hexanuclear clusters for the design and synthesis of highly-connected ftw-MOFs. *Chem. Sci.* **2015**, *6*, 4095−4102.
(42) Jiang, H. L.; Feng, D.; Liu, T. F.; Li, J. R.; Zhou, H. C. Pore Surface Engineering with Controlled Loadings of Functional Groups via Click Chemistry in Highly Stable Metal-Organic Frameworks. *J. Am. Chem. Soc.* **2012**, *134*, 14690−14693.
(43) Xue, D. X.; Cairns, A. J.; Belmabkhout, Y.; Wojtas, L.; Liu, Y.; Alkordi, M. H.; Eddaoudi, M. Tunable Rare-Earth fcu-MOFs: A Platform for Systematic Enhancement of CO_2 Adsorption Energetics and Uptake. *J. Am. Chem. Soc.* **2013**, *135*, 7660−7667.
(44) Czepirski, L.; Jagiello, J. Virial-type thermal equation of gas-solid adsorption. *Chem. Eng. Sci.* **1989**, *44*, 797−801.
(45) Sumida, K.; Rogow, D. L.; Mason, J. A.; McDonald, T. M.; Bloch, E. D.; Herm, Z. R.; Bae, T. H.; Long, J. R. Carbon Dioxide Capture in Metal-Organic Frameworks. *Chem. Rev.* **2012**, *112*, 724−781.
(46) Couck, S.; Denayer, J. F.; Baron, G. V.; Rémy, T.; Gascon, J.; Kapteijn, F. An Amine-Functionalized MIL-53 Metal-Organic Framework with Large Separation Power for CO_2 and CH_4. *J. Am. Chem. Soc.* **2009**, *131*, 6326−6327.
(47) Liu, J.; Benin, A. I.; Furtado, A. M. B.; Jakubczak, P.; Willis, R. R.; LeVan, M. D. Stability Effects on CO_2 Adsorption for the DOBDC Series of Metal-Organic Frameworks. *Langmuir* **2011**, *27*, 11451−11456.
(48) Fracaroli, A. M.; Furukawa, H.; Suzuki, M.; Dodd, M.; Okajima, S.; Gándara, F.; Reimer, J. A.; Yaghi, O. M. Metal-Organic Frameworks with Precisely Designed Interior for Carbon Dioxide Capture in the Presence of Water. *J. Am. Chem. Soc.* **2014**, *136*, 8863−8866.
(49) Ohmichi, M.; Pang, L.; Ribon, V.; Gazit, A.; Levitzki, A.; Saltiel, A. R. The Tyrosine Kinase Inhibitor Tyrphostin Blocks the Cellular Actions of Nerve Growth Factor. *Biochemistry* **1993**, *32*, 4650−4658.
(50) Jeong, N. C.; Lee, J. S.; Tae, E. L.; Lee, Y. J.; Yoon, K. B. Acidity Scalefor Metal Oxides and Sanderson's Electronegativities of Lanthanide Elements. *Angew. Chem., Int. Ed.* **2008**, *47*, 10128−10132.

DOI: 10.1021/acs.inorgchem.7b03084
Inorg. Chem. 2018, 57, 2193−2198